

1
2
3
4
5
6
7
8
9
10
11
12
13
14
15
16
17
18
19
20
21
22
23
24
25
26
27
28
29
30
31
32
33
34
35
36
37
38
39
40
41
42
43
44
45
46
47
48
49
50
51
52
53
54
55
56
57
58
59
60
61
62

Title: Pan-tropical climate interactions

Authors: Wenju Cai^{1,2}, Lixin Wu^{*,1}, Matthieu Lengaigne^{3,4}, Tim Li⁵, Shayne McGregor^{6,7}, Jong-Seong Kug⁸, Jin-Yi Yu⁹, Malte F. Stuecker^{10,11}, Agus Santoso^{2,12}, Xichen Li¹³, Yoo-Geun Ham¹⁴, Yoshimitsu Chikamoto¹⁵, Benjamin Ng², Michael J. McPhaden¹⁶, Yan Du^{17,18}, Dietmar Dommenget¹⁹, Fan Jia²⁰, Jules B. Kajtar²¹, Noel Keenlyside^{22,23}, Xiaopei Lin¹, Jing-Jia Luo²⁴, Marta Martín-Rey^{25,26}, Yohan Ruprich-Robert²⁷, Guojian Wang^{1,2}, Shang-Ping Xie²⁸, Yun Yang²⁹, Sarah M. Kang³⁰, Jun-Young Choi¹⁴, Bolan Gan¹, Geon-Il Kim⁸, Chang-Eun Kim⁸, Sunyoung Kim⁸, Jeong-Hwan Kim¹⁴, Ping Chang³¹

Affiliations:

1. Physical Oceanography Laboratory/CIMST, Ocean University of China and Qingdao National Laboratory for Marine Science and Technology, Yushan Road, Qingdao 266003, China
2. Centre for Southern Hemisphere Oceans Research (CSHOR), CSIRO Oceans and Atmosphere, Hobart 7004, Australia
3. Sorbonne Universités (UPMC, Univ Paris 06)-CNRS-IRD-MNHN, LOCEAN Laboratory, IPSL, 75005 Paris, France
4. Indo-French Cell for Water Sciences, IISc-NIO-IITM-IRD Joint International Laboratory, National Institute of Oceanography, 403004 Dona Paula, India
5. Department of Atmospheric Sciences, University of Hawaii at Manoa, 2525 Correa Road, Honolulu, HI 96825, USA
6. School of Earth Atmosphere and Environment, Monash University, Australia
7. ARC Centre of Excellence for Climate Extremes, Monash University, Australia
8. Division of Environmental Science & Engineering, Pohang University of Science and Technology (POSTECH), 77 Cheonam-Ro Nam-Gu Pohang 37673, South Korea
9. Department of Earth System Science, University of California at Irvine, 3315 Croul Hall, Irvine, CA 92697-3100, USA
10. Center for Climate Physics, Institute for Basic Science (IBS), Busan 46241, Republic of Korea
11. Pusan National University, Busan 46241, Republic of Korea
12. Australian Research Council (ARC) Centre of Excellence for Climate Extremes, Level 4 Mathews Building, The University of New South Wales, Sydney 2052, Australia
13. Institute of Atmospheric Physics, Chinese Academy of Sciences, China
14. Department of Oceanography, Chonnam National University, 77, Yongbong-ro, But-gu, Gwangju, 61186, South Korea
15. Department of Plants, Soils and Climate, Utah State University, 4820 Old Main Hill, Logan, UT 84322, USA
16. NOAA/Pacific Marine Environmental Laboratory, Seattle, WA 98115, USA
17. State Key Laboratory of Tropical Oceanography, South China Sea Institute of Oceanology, Chinese Academy of Sciences, Guangzhou, 510301, China.
18. University of Chinese Academy of Sciences, Beijing, 100049, China
19. ARC Centre of Excellence for Climate Extremes, School of Earth, Atmosphere and Environment, Monash University, Rainforest Walk 9, Clayton, VIC 3800, Australia
20. Key Laboratory of Ocean Circulation and Waves, Institute of Oceanology, Chinese Academy of Sciences, Qingdao 266071, China
21. College of Engineering, Mathematics, and Physical Sciences, University of Exeter, North Park Road, Exeter, EX4 4QE, UK
22. Geophysical Institute, University of Bergen and Bjerknes Centre for Climate Research, Allegaten 70, 5007 Bergen, Norway
23. Nansen Environmental and Remote Sensing Center and Bjerknes Centre for Climate Research, Bergen
24. Key Laboratory of Meteorological Disaster, Ministry of Education (KLME)/Joint International Research Laboratory of Climate and Environmental Change (ILCEC)/Collaborative Innovation Center on Forecast and Evaluation of Meteorological Disasters (CIC-FEMD), Nanjing University of Information Science and Technology, Nanjing, 210044, People's Republic of China.
25. UMR5318 CECI CNRS-CERFACS, Toulouse, Toulouse, France
26. Departamento de Física de la Tierra y Astrofísica, Universidad Complutense de Madrid (UCM), Madrid, Spain
27. Barcelona Supercomputing Center, Barcelona, Spain
28. Scripps Institution of Oceanography, University of California, San Diego, 9500 Gilman Drive, La Jolla, CA 92093, USA
29. College of Global Change and Earth System Science, Beijing Normal University, Beijing 100875, China
30. School of Urban and Environmental Engineering, Ulsan National Institute of Science and Technology, Ulsan 44919, Republic of Korea
31. Department of Oceanography, 3146 TAMU, Texas A&M University, College Station, TX 77843, USA

***Correspondence to: Lixin Wu, Physical Oceanography Laboratory/CIMST, Ocean University of China and Qingdao National Laboratory for Marine Science and Technology, Yushan Road, Qingdao 266003, China (E-mail: lxwu@qnlm.ac)**

63 **One sentence summary:** A complete understanding of how the tropics affect global climate
64 requires a unified perspective of inter-basin interactions.

65 **Abstract:** The El Niño-Southern Oscillation (ENSO), which originates in the Pacific, is the
66 strongest and most well-known mode of tropical climate variability. Its reach is global and it can
67 force climate variations of the tropical Atlantic and Indian Oceans by perturbing the global
68 atmospheric circulation. Less appreciated is how the tropical Atlantic and Indian Oceans affect the
69 Pacific. Especially noteworthy is the multi-decadal Atlantic warming that began in the late 1990s,
70 as recent research suggests that it has influenced Indo-Pacific climate, the character of the ENSO
71 cycle, and the hiatus in global surface warming. Discovery of these pan-tropical interactions
72 provides a pathway forward for improving predictions of climate variability in the current climate,
73 and for refining projections of future climate under different anthropogenic forcing scenarios.

74 **Main text:** Tropical ocean-atmosphere interactions significantly affect the global climate system
75 with socio-economic impacts that are felt worldwide. The El Niño-Southern Oscillation (ENSO)
76 (see **Box 1** for key concepts) in the Pacific is the most prominent and consequential climate
77 variation on the planet, but there are other patterns of climate variability in the tropical Indian
78 and Atlantic Oceans that also have societal impacts. How these various patterns of climate
79 variability interact with one another is an ongoing matter of debate. In particular, the prevailing
80 view for many years was that variability in the Pacific had major impacts on the other two tropical
81 ocean basins, which in turn had only limited influence on the evolution of climate variability in the
82 Pacific. Multiple lines of new evidence now suggest that this view is incomplete and inaccurate.

83 Discovery of the Indian Ocean Dipole (IOD) (1, 2), for example, highlighted a climate scale
84 fluctuation in the Indian Ocean that arises through ocean-atmosphere interactions somewhat
85 similar to those that generate Pacific ENSO events. The consensus view originally was that ENSO
86 was largely responsible for energizing the IOD through changes in the Walker circulation, but we
87 now realize that year-to-year variations in Indian Ocean sea surface temperature (SST), related to
88 the IOD and particularly the Indian Ocean Basin (IOB) mode, can significantly feed back onto the
89 evolution of ENSO (3, 4). Similarly, in the past decade, we have come to appreciate how important
90 it is to understand the great diversity in amplitude, spatial pattern, and duration of individual

91 ENSO events because of how sensitive ENSO climate impacts are to the details of SST structure
92 and evolution (5, 6). We have also begun to recognize that the dynamics that govern this diversity
93 involve two-way interactions between the Atlantic and Pacific Oceans (7-10). In addition, the
94 hiatus in global surface warming during the late 1990s was associated with an unprecedented
95 intensification of the Pacific trade wind system and cooling of the tropical eastern Pacific (11, 12).
96 Although some studies highlight the role of Pacific only ocean-atmosphere feedbacks in forcing the
97 intensified trade winds (13, 14), and there is the possibility that changes in external forcing (e.g.,
98 aerosols) might have contributed to this intensification (15), other studies suggest that a complete
99 explanation may need to invoke forcing from decadal warming trends over the tropical Atlantic (16,
100 17) and Indian Oceans (17, 18) since the late 1990s.

101 The idea of pan-tropical interactions is not new (19) and such interactions should be expected
102 because the three tropical basins are connected via the atmospheric circulation. Recent evidence
103 suggests that these interactions are vigorous, and that the three tropical oceans are more tightly
104 connected than previously thought (16, 17). There is emerging evidence, for example, that in the
105 post-2000 period, the Atlantic Ocean exerted considerable influence on the Pacific and Indian
106 Oceans (7, 8, 10, 16, 17), impacting variability on interannual to decadal timescales. Specifically,
107 this Atlantic influence contributed to decadal changes in ENSO properties and to the hiatus in
108 surface global warming. However, fully-coupled climate models do not generate the observed
109 warming hiatus and the associated changes in tropical variability, in part due to severe systematic
110 biases in the Atlantic (20-22).

111 Interactions with higher latitudes can also influence the character of seasonal to decadal timescale
112 variability in the tropics and there is extensive literature on this topic (23, 24). Our purpose here
113 though is to review recent advances in our understanding of the dynamics of pan-tropical
114 interactions, including their decadal fluctuations, implications for seasonal and multi-year
115 predictions, and future climate projections. We show that the linkages between the Indian, Pacific,
116 and Atlantic Oceans can be exploited for improved seasonal to decadal climate predictions. To fully
117 realize the potential for improved prediction, climate model systematic errors, especially in the
118 tropical Atlantic, must be significantly reduced. Reducing these errors would also greatly increase
119 our confidence in model projections of future climate in the tropics.

120 **Indo-Pacific interactions**

121 The Pacific Ocean and the Indian Ocean are connected through the atmosphere, via the Walker
122 circulation (19) (**Fig. 1A**), and through the ocean via the passages of the Indonesian Archipelago
123 (25). ENSO-induced changes in the Walker circulation often lead to an SST dipole pattern called
124 the IOD (1, 2), followed by a basin-scale warming (26) named the IOB mode (27). This canonical
125 evolution contributed to the perception that the Indian Ocean is slave to the Pacific, but new
126 research revealed a more dynamic Indian Ocean and its active role in shaping Pacific climate.

127 Along with reduced summer monsoon rainfall over the Indian subcontinent (28) a developing El
128 Niño can trigger a positive IOD by inducing easterlies over the equatorial Indian Ocean in boreal
129 summer (29) (**Fig. 1B**), but the IOD can occur independently of (30), and impact on (4), ENSO. An
130 IOD event usually develops in boreal summer, peaks in fall, and decays rapidly in the beginning
131 of winter. A positive Bjerknes feedback (**Box 1**) fosters the IOD development (1, 2). At its positive
132 phase, cold anomalies in the eastern Indian Ocean and warm anomalies in the western Indian
133 Ocean drive equatorial easterly wind anomalies in the central Indian Ocean that enhance the
134 anomalous temperature difference in a positive feedback (**Fig. 1C**), that can occur without ENSO.
135 Because the IOD is accompanied by a zonal dipole in atmospheric convection (**Fig. 1C**), its net
136 effect on the Western Pacific winds, and consequently on ENSO, is uncertain (31). However, strong
137 positive IODs may induce anomalous westerly winds in the western Pacific, contributing to El Niño
138 development (31, 32) (**Fig. 1D**). Thus although the observed statistical ENSO-IOD relationship
139 appears consistent with the IOD being a response to ENSO (33), the IOD is in part independent of
140 ENSO and has the potential to increase ENSO prediction lead times (3, 4).

141 The IOB, which is the dominant mode of interannual Indian Ocean SST variability, and stronger
142 in variance than the IOD, commences its development in boreal winter. An IOB warming is largely
143 driven by reduced surface evaporation and increased downward shortwave radiation in response
144 to El Niño remote forcing (26). It usually reaches its maximum amplitude in boreal spring (26),
145 about one season after the mature phase of ENSO (**Fig. 1E**). However, the IOB is not simply a
146 passive response to ENSO either. ENSO excites the IOB like a battery charging a capacitor, but
147 the IOB can exert its climatic influence beyond the lifetime of an ENSO event like a discharging

148 capacitor (27, 34). In the southwest Indian Ocean where the thermocline is shallow (35, 36),
149 westward propagating downwelling Rossby waves in response to the weakened Walker circulation
150 induce SST warming beginning in boreal fall (35). This warming strengthens atmospheric
151 convection and triggers an asymmetric wind anomaly pattern across the equatorial Indian Ocean
152 in boreal spring (36) (**Fig. 1E**). The anomalous wind pattern contributes to a subsequent warming
153 in the north Indian Ocean through summer, which is in turn strengthened by a positive feedback
154 with the northwest Pacific anomalous anticyclone by radiating an atmospheric Kelvin wave (34)
155 (**Fig. 1F**). This coupled inter-basin mode leads to a strengthened Asian summer monsoon in the
156 post-El Niño summer (28, 37).

157 In contrast to the reinforcing role of a positive IOD, an IOB warming, though forced by El Niño,
158 hastens El Niño's demise. As an El Niño matures, IOB warming induces enhanced convection over
159 the Indian Ocean which in turn enhances the northwest Pacific anomalous anticyclone and
160 easterly anomalies over the equatorial western Pacific (3) (**Fig. 1, D and E**). The advent of easterly
161 surface wind anomalies from boreal winter to the following summer expedites the El Niño demise
162 (3, 38). The IOB hence damps ENSO variability and contributes to its biennial timescale, as
163 corroborated by climate model experiments where the Indian Ocean is decoupled from the Pacific
164 (39-42). Despite their contrasting roles, a long-lasting IOB warming after a strong positive IOD
165 may lead to a fast phase transition of El Niño to La Niña (43). This is because an abrupt wind
166 change is fostered by the sequence of events that starts with a positive IOD contributing to an El
167 Niño, which in turn drives a strong IOB warming that then enhances central Pacific cooling (43,
168 44).

169 The relationship between variability of the two oceans is time-varying and asymmetric about their
170 positive and negative phases. ENSO exhibits a variety of spatial SST patterns, which have
171 different consequences on the Walker circulation response (45). The frequent occurrence of central
172 Pacific (CP) El Niño events in recent decades (46), which tend to have smaller amplitudes than
173 corresponding eastern Pacific (EP) El Niño events, might explain a recent weakening of the ENSO-
174 IOD relationship (45, 47). Because SST and atmospheric deep convection anomalies over the Indo-
175 Pacific are larger during El Niño compared to La Niña, an IOB warming is more efficient at
176 influencing west Pacific wind anomalies during El Niño than La Niña. As such, the IOB warming

177 is more efficient in contributing to the demise of El Niño than an IOB cooling to the demise of La
178 Niña (38, 48). This asymmetric response contributes to ENSO duration asymmetry, with La Niña
179 typically lasting longer than El Niño (48).

180 Although changes in the atmospheric Walker circulation dominate ENSO interactions with both
181 the IOB and the IOD, the oceanic pathway across the Indonesian Seas has a prominent role in
182 Indo-Pacific exchanges. This flow, termed the Indonesian Throughflow, is a major component of
183 the global ocean circulation and plays a key role in the transport of mass, heat, and salt from the
184 Pacific to the Indian Ocean (25). Decadal changes in the Throughflow affect the background
185 thermal structure of the Indian Ocean, which can in turn modulate IOD characteristics (49).
186 During the recent hiatus in global surface warming, increased heat uptake in the Pacific was
187 shown to be partly transported to the Indian Ocean via the Throughflow (50). However, recent
188 studies suggest that the dynamics of the hiatus per se may involve interactions between the
189 Atlantic and Indo-Pacific (12, 16, 17).

190 **Atlantic and Indo-Pacific interactions**

191 Modeling and observational evidence suggests that two-way interactions between the tropical
192 Atlantic and Pacific operate on interannual timescales (10, 51). Tropical Atlantic variability, in
193 part forced by ENSO, feeds back onto ENSO. For example, decoupling the Atlantic Ocean in
194 otherwise fully coupled models generally leads to a stronger ocean-atmosphere coupling strength
195 in the equatorial Pacific, a shift to a lower ENSO frequency, and an increase in ENSO variance
196 (10, 19, 39, 41, 42, 52, 53).

197 El Niño-induced atmospheric heating forces the tropical Atlantic through two distinct pathways,
198 one of which is tropical and the other of which is extratropical. The tropical pathway involves a
199 weakening of the Walker circulation that in turn generates anomalous descending motion over the
200 tropical Atlantic (24, 52). The extratropical pathway involves excitation of the Pacific–North
201 American (PNA) pattern with an anomalously low surface pressure center over the western
202 subtropical Atlantic (54) (red circles, **Fig. 1D**). As a result, the north tropical Atlantic (NTA; 10°N–
203 20°N) (northern black box, **Fig. 2A**) warms significantly, peaking in boreal spring 3–5 months after
204 an El Niño matures in December (55) (**Fig. 1E**). This NTA warming arises from reduced surface

205 latent heat flux due to a weakening of north-easterly trades, associated with a PNA low pressure
206 anomaly to the north, an anomalous descent to the south, and a sustained wind-evaporative-SST
207 (WES) effect (26) (**Box 1; Fig. 1D**). Models appear able to capture this Atlantic response (56, 57),
208 but there is uncertainty as to the relative role of the tropical and extratropical processes. This is
209 because the weakened northeasterly trades can be caused by the anomalous Walker and local
210 Hadley cells (58), a Gill-type response to Amazonian heating (59) (**Box 1**), or a tropospheric
211 temperature warming in response to El Niño (24, 60).

212 In turn, NTA anomalous warming has been suggested to impact ENSO. An NTA warming in boreal
213 spring excites an atmospheric Rossby wave that propagates westward, causing northeasterly wind
214 anomalies over the subtropical north-eastern Pacific (8) (**Fig. 2A**). This can generate cold SST and
215 low rainfall anomalies in subsequent seasons, inducing a low-level anticyclone further to the west
216 (**Fig. 2B**). The associated easterly wind anomalies in the western equatorial Pacific might in turn
217 initiate a La Niña (**Fig. 2C**). An atmospheric Kelvin wave response to the NTA warming can also
218 induce easterly anomalies through the Indian Ocean (61) (**Fig. 2, A and B**). This NTA forcing
219 tends to favor the CP type of ENSO (8, 10), consistent with an extratropical Pacific forcing of CP
220 ENSO events (62).

221 Another center of inter-basin interactions is the equatorial Atlantic (southern black box, **Fig. 2B**),
222 where the Atlantic Niño dominates (63). ENSO's influence on the equatorial Atlantic is not robust
223 however, with only a weak concurrent correlation between ENSO and the equatorial Atlantic SST
224 (55, 64). During El Niño, a weakening Walker circulation and the associated easterly wind
225 anomalies along the equator in the Atlantic (**Fig. 1B**) tend to generate cold anomalies through the
226 Bjerknes positive feedback (65). However, this cooling may be offset by either tropospheric
227 warming in response to El Niño (66) and/or by oceanic downwelling Kelvin waves induced by a
228 meridional SST gradient due to warming in the NTA, propagating into the region (67). These
229 competing effects may contribute a weak influence of ENSO on equatorial Atlantic SST and to the
230 concurrent weak relationship between ENSO in the Pacific and the equatorial Atlantic SST.

231 By contrast, influence of the equatorial Atlantic on ENSO is robust since the 1970s, as reflected in
232 a statistically significant negative correlation when an equatorial Atlantic Niño/Niña leads a

233 Pacific La Niña/El Niño by two seasons (64, 68-70). For example, an Atlantic Niño, which peaks in
234 boreal summer, induces anomalous ascending motion over the Atlantic and anomalous subsidence
235 over the central Pacific (**Fig. 2B**). The associated easterly wind anomalies over the central and
236 western equatorial Pacific excite an oceanic upwelling Kelvin wave that triggers the Pacific
237 Bjerknes feedback, conducive to development of a La Niña event six months later (71) (**Fig. 2C**).

238 The role of the tropical Atlantic on ENSO variability is corroborated by pacemaker climate model
239 experiments. When observed historical SST is prescribed over the tropical Atlantic, models are
240 able to reproduce the observed impact on ENSO (**Fig. 2, D to F**) (69-71). Figure 2 is based on the
241 ensemble average of a five-member ensemble pacemaker experiment over the period of 1980-2005,
242 in which full coupling is permitted everywhere except in the tropical Atlantic (30°S-30°N), where
243 SSTs are nudged to observations. This, along with other pacemaker experiments, shows that the
244 tropical Atlantic contributes to approximately 25% of Indo-Pacific SST variance (69-71). However,
245 as ENSO's impact on Atlantic Niño is not as robust as on the NTA, the two-way interaction of the
246 Pacific with the NTA is stronger than with the equatorial Atlantic. An El Niño event during boreal
247 winter can induce NTA warming in the ensuing spring (**Fig. 1E**), in turn contributing to the
248 transition to a La Niña (**Fig. 2, C and F**) (10). This interaction constitutes a delayed negative
249 feedback for ENSO, shortening ENSO periodicity (42) as the IOB does (3, 38).

250 This two-way interaction between NTA variability and Pacific ENSO has been reported to have
251 strengthened since the late 1990s, coincident with the Atlantic Multi-decadal Variability (AMV,
252 see **Box 1**) switch to a positive phase and an increasing tendency for biennial CP ENSO events (8,
253 10). The positive phase of the AMV provides a warmer background NTA SST, which favors deep
254 convection and a strengthening of the NTA influence on the Pacific. Such a feedback appears to be
255 less active during a negative AMV phase, when the impact of the equatorial Atlantic tends to be
256 stronger (72) because of a southward shift of the Inter-Tropical Convergence Zone (ITCZ). This
257 shift leads to a stronger and wider westward extension of equatorial Atlantic interannual
258 variability, facilitating a strong influence on the central and eastern Pacific (73, 74). In addition,
259 winds associated with a negative AMV phase may cause the tropical Pacific mean thermocline to
260 shoal, increasing the mean stratification to favor enhanced ENSO variability (75).

261 The impact of the tropical Atlantic extends to the Indian Ocean and the Western Pacific, affecting
262 monsoons over these regions. An Atlantic Niño forces a Gill-type quadrupole response with a low-
263 level anticyclone located over India and the western North Pacific suppressing the monsoon
264 circulation (76, 77). The competing impacts of the Atlantic and ENSO on the monsoons may explain
265 the post-mid 1970s collapse of the ENSO-Indian monsoon relationship, in which a drier than
266 normal monsoon typically precedes an El Niño peak (76, 77). An alternative hypothesis is that
267 observed decadal changes in the ENSO-Indian monsoon relationship are explained by the noise in
268 the system (78).

269 **Rise of the tropical Atlantic influence**

270 As discussed in Sections 2 and 3, ENSO characteristics can be significantly influenced by SST
271 anomalies in the Indian and Atlantic Oceans. In this section, we describe similar inter-basin
272 interactions that operate on decadal timescales, highlighting how interaction between the Atlantic
273 and Indian Oceans with the Pacific Ocean changed in the 1990s. The Atlantic-Pacific connection
274 now appears as the most prominent inter-basin interaction.

275 The IPO phase transition that occurred in the late 1990s has led to an unprecedented acceleration
276 of the Walker circulation and contributed to the recent hiatus in global mean surface temperature
277 (11, 16, 17, 79), but what caused the IPO itself to change phase is not clear. The associated change
278 in wind stress curl increases ocean heat uptake (12, 80, 81) and the strengthened Walker
279 circulation intensifies the ITF, distributing the heat through the upper eastern Indian Ocean and
280 the Indonesian Seas (25, 80). Evidence suggests that the dynamics of these Pacific changes are not
281 entirely internal to the Pacific, and forcing from the Indian and Atlantic Oceans needs to be
282 considered (12, 16, 82).

283 On decadal and multi-decadal timescales, the Indian Ocean also influences the Pacific through the
284 tropical atmospheric bridge (3, 38). Surface warming in the Indian Ocean, relative to the Pacific
285 basin, leads to overlying deep convection and associated Walker circulation changes across the
286 Indo-Pacific region that increase the surface easterlies in the western and central Pacific (18) (**Fig.**
287 **3A**). Because the temperature threshold for deep convection increases with the mean tropical
288 temperature (83), the relative warming can be represented by a tropical Indian-minus-Pacific

289 trans-basin SST gradient to remove the mean tropical warming (blue curve, **Fig. 3C**). The trans-
290 basin gradient displays a good relationship with the Pacific winds (black curve, **Fig. 3C**), which
291 eventually drives a La Niña-like state through the Pacific Bjerknes feedback. But this relationship
292 has weakened in recent decades (82, 84), as indicated by reduced coherence between trends of
293 Indian-minus-Pacific inter-basin SST gradients and equatorial central Pacific zonal wind stress
294 (blue and black curves, **Fig. 3C**), but whether stochastic forcing plays a role is not clear (78).

295 Relative to the Indian Ocean, the Atlantic Ocean appears to have a greater influence on Pacific
296 decadal variability in recent decades, and this can be conducted via extratropical and tropical
297 pathways. One proposed extratropical pathway is that a warm North Atlantic SST anomaly
298 weakens storm tracks over the North Atlantic and the North Pacific mid-latitudes, generating an
299 anomalous North Pacific high pressure and a PNA pattern over the North Pacific (85). Another
300 proposed extratropical connection is that warming in the North Atlantic enhances local convection
301 but increases subsidence in the North Pacific, contributing to the high pressure over the
302 subtropical North Pacific, which decreases the wind speed of the subtropical North Pacific
303 westerlies and induces a north-western subtropical Pacific warming through the WES effect and
304 other processes (86). However, recent research suggests that these extratropical pathways play a
305 minor role compared to the tropical pathway (87). Tropical Atlantic warming drives a convective
306 response and an associated diabatic atmospheric heating anomaly, the magnitude of which is
307 dependent on the magnitude of Atlantic SST anomalies relative to the tropical mean SSTs. This
308 difference can be represented by a tropical Atlantic-minus-Pacific trans-basin SST gradient (red
309 curve, **Fig. 3C**), also called Trans-Basin Variability (TBV) (16, 88). The tropical Atlantic diabatic
310 heating leads to a Gill-type (**Box 1**) response that results in an anomalous rising Walker circulation
311 branch over the tropical North Atlantic and an anomalous sinking branch over the tropical central
312 and eastern Pacific (16, 17, 75, 87, 89, 90) (**Fig. 3B**). The associated surface circulation anomalies
313 lead to WES-induced surface cooling in the eastern/central Pacific and warming in the off-
314 equatorial western Pacific. These processes intensify the Pacific Walker circulation through the
315 Bjerknes feedback and lead to a La Niña-like state within the Pacific (16, 17), mechanisms similar
316 to those that trigger La Niña by the equatorial Atlantic warming on interannual timescales (91).

317 Tropical Atlantic forcing of the Pacific can also be enhanced through the Indian Ocean, whereby
318 the Atlantic Ocean-forced Indo-Pacific easterly wind anomalies of the Gill-type response generate
319 the Indo-Pacific warming via the WES effect (17). This Indo-western Pacific warming in turn
320 intensifies the La Niña-like response by enhancing the Pacific trade winds through a mechanism
321 similar to the IOB's role in the transition from El Niño to La Niña (3, 38) (**Fig. 3D**).

322 The Atlantic influence in recent decades can be reproduced in coupled simulations forced with SST
323 anomalies only in the tropical Atlantic (16, 17). This includes a La Niña-like state that is shown to
324 lead to a higher frequency of La Niña than El Niño events (87), which is consistent with
325 observations since 2000. Similar coupled simulations forced with Indian Ocean SST anomalies find
326 only a limited role for the recent observed Indian Ocean warming alone (16, 17). Thus, since the
327 late 1990s, the tropical Atlantic warming appears to have affected the entire tropics, while the
328 induced Pacific response has contributed to the global temperature hiatus and its many regional
329 impacts (11). However, it is not clear whether, or to what extent, the rise of the Atlantic influence
330 is related to the loss of connectivity between the Indian and Pacific Oceans. It remains an open
331 question as to what caused the recent (1992–2011) decadal warming trend in the tropical Atlantic
332 or what is the relative importance of internal variability and external forcing (92).

333 **Implications of pan-tropical interactions**

334 Classical prediction frameworks rely only on internal Pacific precursors such as the equatorial
335 Pacific warm water volume (93, 94), which leads the ENSO SST signal by 6-9 months. The fact
336 that ENSO properties and the Pacific decadal changes are affected by the Indian and Atlantic
337 Oceans offers additional precursors (green and purple boxes, **Fig. 4, A to C**). However, these
338 precursors are not well simulated by the majority of climate models (**Fig. 4, D to F**).

339 Knowledge of Indian Ocean conditions has been shown to improve ENSO forecasts (4, 32).
340 Incorporating information from an extreme positive IOD leads to improved prediction of the
341 1994/95 CP El Niño and of the intensity of the extreme El Niño in 1997/98; incorporating
342 information of the IOD and the IOB combined improves the predicted ENSO evolution (32),
343 particularly the phase transition from an El Niño to La Niña (4). In a similar vein, knowledge of
344 Atlantic SST conditions improves ENSO prediction in dynamical and statistical models (90, 95,

345 96). Hindcast experiments with additional equatorial Atlantic SST information increases
346 predictability of the major 1982/1983 and 1997/1998 El Niño events (95). Further, NTA SST offers
347 an independent precursor for ENSO. For example, since 1980, three out of the four cases of boreal
348 spring NTA cooling (i.e. 1986, 1994, and 2009) were followed by a CP El Niño in winter, and all
349 cases of boreal spring NTA warming (i.e., 1980, 1988, 1998, and 2010) were followed by a Pacific
350 La Niña (91). Since the NTA and the equatorial Atlantic contribute to predictive skill over the
351 central and eastern Pacific, respectively (91), these Atlantic precursors may offer potential for
352 prediction of ENSO diversity.

353 Combining Indian and Atlantic Ocean precursors (**Fig. 4, A to C**) with those internal to the Pacific
354 may considerably increase ENSO prediction skill (53) (**Fig. 4G**), particularly in recent decades
355 (**Fig. 4H**). Enhanced ENSO prediction as a result of incorporating inter-basin precursors, in turn,
356 could contribute to Atlantic and Indian Ocean climate prediction. Dynamical prediction
357 experiments show that incorporating tropical Pacific information greatly enhances the predictive
358 skill of the IOD and the IOB (97) and the tropical Atlantic climate (98). Understanding pan-tropical
359 interactions is therefore crucial for improving prediction of interannual tropical climate, its
360 atmospheric teleconnections, and its global impacts.

361 The Atlantic contribution to Indo-Pacific climate predictability extends to multi-year timescales.
362 Although internally generated decadal climate variability in the extratropical North Atlantic and
363 North Pacific is predictable by up to half a decade in advance (99, 100), such skill is still elusive
364 for tropical climate. The influence of tropical Atlantic SST variability associated with the AMV can
365 be utilized for Pacific decadal prediction (87, 101). Such prediction skill is achieved via a global
366 reorganization of the Walker circulation, which can be represented by a TBV index measuring the
367 tropical SST gradient between the Pacific and the other two oceans (101). The index displays
368 predictability at multi-year lead times with contributions from the Atlantic and Indian Oceans. In
369 particular, the Atlantic influence considerably increases decadal predictability in the central
370 Pacific SST (88).

371 Most state-of-the-art climate models fail to reproduce the observed pan-tropical interactions. In
372 addition to an underestimated influence on ENSO from the NTA (102), equatorial Atlantic

373 variability (22), and the IOD (103) (**Fig. 4, D to F**), the majority of models produce too weak of a
374 relationship between decadal trends of the TBV and Pacific trade winds (21). In fact, the
375 relationship between trends of tropical Atlantic SST and equatorial Pacific trade winds is opposite
376 to that observed in most models (21). This unrealistic relationship is partially associated with a
377 bias in the tropical Atlantic mean state (20, 21), which features a weaker than observed, or even
378 reversed, west-minus-east equatorial SST gradient. This bias leads to a weak convective response
379 to Atlantic SST anomalies and a weaker Walker circulation response that is shifted to the east, the
380 consequence of which is an unrealistic relationship between the Atlantic and Pacific (20).

381 Systematic model errors in pan-tropical interactions may be in part responsible for the inability of
382 models to simulate the recent global warming hiatus (20, 103), in which greenhouse warming was
383 offset by a cooling trend in the tropical Pacific (11, 12). Further, faster warming in the Indian
384 Ocean than the Pacific, as observed over the past decades, is conducive to easterlies in the western
385 Pacific (18, 84), through mechanisms similar to those operating on interannual timescales
386 associated with an IOB warming (3). Given that Indian Ocean warming is at least in part driven
387 by Atlantic warming in recent decades (17), systematic errors in the Atlantic-Pacific relationship
388 might have suppressed important processes. The suppression of these processes may be responsible
389 for the projected greater warming in the equatorial eastern Pacific under greenhouse warming.
390 Therefore, correcting the biases in the Atlantic-Pacific relationship may lead to reduced eastern
391 equatorial Pacific warming in climate projections.

392 Without properly accounting for Atlantic-Pacific and Atlantic-Indian Ocean interactions, the
393 potential for an Atlantic warming-induced Pacific cooling is muted. Thus, this bias may have far
394 reaching implications for projections of future climate, particularly in Pacific mean state change.
395 For example, models exhibiting a stronger correlation between decadal trends of the TBV index
396 and equatorial Pacific trade winds tend to project a weakened future warming in the tropical
397 Pacific compared to those with a weaker decadal coupling (**Fig. 5, A and B**), supporting the notion
398 that a realistic representation of pan-tropical interactions in climate models may substantially
399 modify the projected Pacific mean state change (22).

400 **Summary and pathway forward**

401 Pan-tropical interactions are more vigorous than previously thought and the three ocean basins
402 are more tightly interconnected than previously realized. In addition to well-known Pacific Ocean
403 influences on the Indian and the Atlantic Oceans, there are highly consequential feedbacks from
404 these two basins on the Pacific on interannual to decadal timescales. For example, a positive NTA
405 SST anomaly in boreal spring can trigger a central Pacific La Niña (8, 10), whereas an equatorial
406 Atlantic Niña in boreal summer can force an EP El Niño (64), thereby contributing to ENSO
407 diversity. Similarly, a positive IOD can favor the onset of El Niño and an El Niño-forced IOB can
408 accelerate the demise of an El Niño and its transition to La Niña (3, 4, 32). Modeling studies
409 suggest that the net impact of the Indian and Atlantic Oceans on the ENSO cycle damps its
410 amplitude and increases its frequency (3, 38, 41, 42).

411 These tropical inter-basin linkages vary significantly on decadal timescales. In particular, tropical
412 warming associated with the positive phase of the AMV over the past two decades represents a
413 major forcing on the Pacific and Indian Oceans (16, 17). This tropical Atlantic warming contributed
414 to an extraordinary intensification of the Pacific trade winds accompanied by surface cooling in the
415 eastern tropical Pacific, an increased ITF heat transport from the Pacific to the Indian Ocean, and
416 an increased sequestration of heat in the Indian Ocean. A warmer Indian Ocean in turn also
417 favored further intensification of the Pacific trade winds through changes in the Walker circulation
418 (17, 84). In this scenario, the tropical Atlantic emerges as pivotal in driving the recent hiatus in
419 global surface warming.

420 Our knowledge of the pan-tropical inter-basin interactions is still in its infancy and many
421 uncertainties exist. Given the relatively short observational record that dates back only to the
422 second half of the 19th century, our ability to clearly define and understand inter-basin
423 interactions across the full range of interannual to decadal and longer timescales is limited. For
424 instance, available observations suggest that the sign of the AMV determines whether the
425 equatorial Atlantic Niño (for negative AMV) or the NTA (for positive AMV) is the most active
426 pathway of influence on the Pacific (74). However, the relative importance of these two Atlantic
427 SST modes in exciting inter-basin teleconnections is largely unknown. Whether these AMV
428 influences are robust and what causes this multi-decadal modulation in inter-basin teleconnections
429 are open questions.

430 Much of the new insight about the tropical Atlantic's role in tropical inter-basin interactions
431 emerges from observations since 2000, when the AMV turned positive and reached its highest
432 value in the instrumental record. It is unclear however what the relative importance of natural
433 climate variability and anthropogenic forcing is in driving this Atlantic warming, whether the
434 recent Atlantic influence on pan-tropical climate is reinforced by anthropogenic forcing, or how
435 inter-basin interactions may affect the climate of the tropics in the future. Climate modeling studies
436 to address these issues are unfortunately compromised by pronounced systematic errors in the
437 tropical Atlantic that severely suppress interactions with the Indian and Pacific Oceans (20-22).
438 These model biases in particular could have a substantial impact on the simulated ENSO
439 characteristics and the Pacific mean state. As a result, there could be considerable uncertainty in
440 future projections of Indo-Pacific climate variability and the background conditions in which it is
441 embedded. Projections based on the current generation of climate models suggest that Indo-Pacific
442 mean state changes will involve slower warming in the eastern than in the western Indian Ocean
443 and a faster warming in the east equatorial Pacific than the surrounding regions (104). Given the
444 presumed strength of the Atlantic influence on the pan-tropics, projections of future climate change
445 could be substantially different if model systematic errors in the Atlantic were corrected.

446 Nevertheless, recent advances in our understanding of the pan-tropical interactions provide
447 valuable guidance for setting research priorities. Among these is the urgent need to reduce model
448 systematic errors in the Atlantic as one key ingredient to enable further progress and there have
449 been efforts to solve this (105). It has been extraordinarily difficult to remedy such errors as we
450 have learned from the Pacific cold tongue and double ITCZ biases, problems for which there has
451 been no solution for decades. Thus, it is essential that we understand the fundamental processes
452 that govern the Atlantic mean state, including interactions between tropical winds, SST, the upper
453 ocean, atmospheric convection, and the role of equatorial ocean mixing. Given the shortness of the
454 instrumental record, studies that take advantage of much longer paleo proxy records can be a
455 valuable source of information on inter-basin interactions in the past. There is also potential for a
456 substantial improvement in ENSO and multi-year predictions, by exploiting the dynamical
457 linkages outside the Pacific basin (88). Success on this front requires a deeper understanding of
458 these linkages to ensure that they are represented as accurately as possible in forecast models.

459 Coordinated modeling studies, including pacemaker experiments, can be used to examine the
460 mechanisms that underpin these tropical inter-basin interactions and their importance relative to
461 extra-tropical influences. Given that the mean state errors in the tropical Atlantic are systematic,
462 flux adjustments in climate models can also be a useful approach for exploring inter-basin
463 interactions in the current climate and potentially in the future as well under differing climate
464 change forcing scenarios. Ultimately, making progress in this enterprise will depend critically on
465 sustained global climate observations, climate model improvements, and theoretical developments
466 that help us to better understand the underlying dynamics of pan-tropical interactions and their
467 climatic impacts.

468 **References and Notes:**

- 469 1. N. H. Saji, B. N. Goswami, P. H. Vinayachandran, T. Yamagata, A dipole mode in the
470 tropical Indian Ocean. *Nature* **401**, 360-363 (1999).
- 471 2. P. J. Webster, M. D. Moore, J. P. Loschnigg, R. R. Lebel, Coupled ocean-atmosphere
472 dynamics in the Indian Ocean during 1997-98. *Nature* **401**, 356-360 (1999).
- 473 3. J.-S. Kug, I.-S. Kang, Interactive feedback between ENSO and the Indian Ocean. *J. Clim.*
474 **19**, 1784–1801 (2006).
- 475 4. T. Izumo, J. Vialard, M. Lengaigne, C. de Boyer Montegut, S. K. Behera, J.-J. Luo, S.
476 Cravatte, S. Masson, T. Yamagata, Influence of the state of the Indian Ocean Dipole on the
477 following year's El Nino. *Nat. Geo.* **3**, 168–172 (2010).
- 478 5. K. Ashok, S. K. Behera, S. A. Rao, H. Weng, T. Yamagata, El Niño Modoki and its possible
479 teleconnection. *J. Geophys. Res.* **112**, C11007 (2007).
- 480 6. Capotondi, A. T. Wittenberg, M. Newman, E. D. Lorenzo, J.-Y. Yu, P. Braconnot, J. Cole,
481 B. Dewitte, B. Giese, E. Guilyardi, F.-F. Jin, K. Karnauskas, B. Kirtman, T. Lee, N.
482 Schneider, Y. Xue, S.-W. Yeh, Understanding ENSO diversity. *Bull. Am. Meteorol. Soc.* **96**,
483 921–938 (2015).
- 484 7. L. Wu, F. He, Z. Liu, Coupled ocean-atmosphere response to north tropical Atlantic SST:
485 Tropical Atlantic Dipole and ENSO. *Geophys. Res. Lett.* **32**, L21712 (2005).
- 486 8. Y.-G. Ham, J.-S. Kug, J.-Y. Park, F.-F. Jin, Sea surface temperature in the north tropical
487 Atlantic as a trigger for El Niño/Southern Oscillation events. *Nat. Geo.* **6**, 112-116 (2013).

- 488 9. F. Jia, L. Wu, B. Gan, W. Cai, Global warming attenuates the tropical Atlantic-Pacific
489 teleconnection. *Sci. Rep.* **6**, 20078 (2016).
- 490 10. L. Wang, J.-Y. Yu, H. Paek, Enhanced biennial variability in the Pacific due to Atlantic
491 capacitor effect. *Nat. Commun.* **8**, 14887 (2017).
- 492 11. Y. Kosaka, S.-P. Xie, Recent global-warming hiatus tied to equatorial Pacific surface
493 cooling. *Nature* **501**, 403-407 (2013).
- 494 12. M. H. England, S. McGregor, P. Spence, G. A. Meehl, A. Timmermann, W. Cai, A. Sen
495 Gupta, M. J. McPhaden, A. Purich, A. Santoso, Recent intensification of wind-driven
496 circulation in the Pacific and the ongoing warming hiatus. *Nat. Clim. Change* **4**, 222-227
497 (2014).
- 498 13. G. A. Meehl, A. Hu, Megadroughts in the Indian Monsoon Region and Southwest North
499 America and a Mechanism for Associated Multidecadal Pacific Sea Surface Temperature
500 Anomalies. *J. Clim.* **19**, 1605-1623 (2016).
- 501 14. R. Farneti, F. Molteni, F. Kucharski, Pacific interdecadal variability driven by tropical-
502 extratropical Interactions. *Clim. Dyn.* **42**, 3337-3355 (2014).
- 503 15. C. Takahashi, M. Watanabe, Pacific trade winds accelerated by aerosol forcing over the
504 past two decades. *Nat. Clim. Change* **6**, 768-772 (2016).
- 505 16. S. McGregor, A. Timmermann, M. F. Stuecker, M. H. England, M. Merrifield, F.-F. Jin, Y.
506 Chikamoto, Recent Walker Circulation strengthening and Pacific cooling amplified by
507 Atlantic warming, *Nat. Clim. Change* **4**, 888-892 (2014).
- 508 17. X. Li, S.-P. Xie, S. T. Gille, C. Yoo, Atlantic induced pan-tropical climate change over the
509 past three decades, *Nat. Clim. Change*. **6**, 275-279 (2016).
- 510 18. J.-J. Luo, W. Sasaki, Y. Masumoto, Indian Ocean warming modulates Pacific climate
511 change. *Proc. Nat. Acad. Sci.* **46**, 18701-18706 (2012).
- 512 19. M. Latif, T. Barnett, Interactions of the tropical oceans. *J. Clim.* **8**, 952-964 (1995).
- 513 20. S. McGregor, M. F. Stuecker, J. B. Kajtar, M. H. England, M. Collins, Model tropical
514 Atlantic biases underpin diminished Pacific decadal variability. *Nat. Clim. Change* **8**, 493-
515 499 (2018).

- 516 21. J. B. Kajtar, A. Santoso, S. McGregor, M. H. England, Z. Baillie, Model under-
517 representation of decadal Pacific trade wind trends and its link to tropical Atlantic bias.
518 *Clim. Dyn.* **50**, 1471-1484 (2018).
- 519 22. F. Kucharski, F. S. Syed, A. Burhan, I. Farah, A. Gohar, Tropical Atlantic influence on
520 Pacific variability and mean state in the twentieth century in observations and CMIP5.
521 *Clim. Dyn.* **44**, 881-896 (2015).
- 522 23. Timmermann, S.-I. An, J.-S. Kug, F.-F. Jin, W. Cai, A. Capotondi, K. Cobb, M. Lengaigne,
523 M. J. McPhaden, M. F. Stuecker, K. Stein, A. T. Wittenberg, K.-S. Yun, T. Bayr, H.-C.
524 Chen, Y. Chikamoto, B. Dewitte, D. Dommenges, P. Grothe, E. Guilyardi, Y.-G. Ham, M.
525 Hayashi, S. Ineson, D. Kang, S. Kim, W. Kim, J.-Y. Lee, T. Li, J.-J. Luo, S. McGregor, Y.
526 Planton, S. Power, H. Rashid, H.-L. Ren, A. Santoso, K. Takahashi, A. Todd, G.-M. Wang,
527 G. Wang, R. Xie, W.-H. Yang, S.-W. Yeh, J. Yoon, E. Zeller, X. Zhang, El Niño–Southern
528 Oscillation complexity. *Nature* **559**, 535–545 (2018).
- 529 24. P. Chang, T. Yamagata, P. Schopf, S. K. Behera, J. Carton, W. S. Kessler, G. Meyers, T.
530 Qu, F. Schott, S. Shetye, S.-P. Xie, Climate fluctuations of tropical coupled systems—the
531 role of ocean dynamics. *J. Clim.* **19**, 5122-5174 (2006).
- 532 25. J. Sprintall, A. L. Gordon, A. Koch-Larrouy, T. Lee, J. T. Potemra, K. Pujiana, S. E. Wijffels,
533 The Indonesian seas and their role in the coupled ocean–climate system. *Nat. Geo.* **7**, 487–
534 492 (2014).
- 535 26. S. A. Klein, B. J. Soden, N. C. Lao, Remote sea surface temperature variations during
536 ENSO: Evidence for a tropical atmospheric bridge. *J. Clim.* **12**, 917–932 (1999).
- 537 27. J. Yang, Q. Liu, S.-P. Xie, Z. Liu, L. Wu, Impact of the Indian Ocean SST basin mode on
538 the Asian summer monsoon. *Geophys. Res. Lett.* **34**, L02708 (2007).
- 539 28. V. Mishra, B. V. Smoliak, D. P. Lettenmaier, J. M. Wallace, A prominent pattern of year-
540 to-year variability in Indian Summer Monsoon Rainfall. *Proc. Nat. Acad. Sci.* **109**, 7213–
541 7217 (2012).
- 542 29. H. Annamalai, R. Murtugudde, J. Potemra, S.-P. Xie, P. Liu, B. Wang, Coupled dynamics
543 over the Indian Ocean: spring initiation of the Zonal Mode. *Deep Sea Res.* **50**, 2305–2330
544 (2003).

- 545 30. S. Fischer, P. Terray, E. Guilyardi, S. Gualdi, P. Delecluse, Two independent triggers for
546 the Indian Ocean Dipole/Zonal Mode in a coupled GCM. *J. Clim.* **18**, 3428–3449 (2005).
- 547 31. H. Annamalai, S. Kida, J. Hafner, Potential impact of the tropical Indian Ocean–
548 Indonesian Seas on El Niño characteristics. *J. Clim.* **23**, 3933–3952 (2010).
- 549 32. J.-J. Luo, R. Zhang, S. K. Behera, Y. Masumoto, Interaction between El Niño and extreme
550 Indian Ocean Dipole. *J. Clim.* **23**, 726–742 (2010).
- 551 33. M. F. Stuecker, A. Timmermann, F.-F. Jin, Y. Chikamoto, W. Zhang, A. T. Wittenberg, E.
552 Widiasih, S. Zhao, Revisiting ENSO/Indian Ocean Dipole phase relationships. *Geophys.*
553 *Res. Lett.* **44**, 2481–2492 (2017).
- 554 34. S.-P. Xie, K. Hu, J. Hafner, H. Tokinaga, Y. Du, G. Huang, T. Sampe, Indian Ocean
555 capacitor effect on Indo–Western Pacific climate during the summer following El Niño. *J.*
556 *Clim.* **22**, 730–747 (2009).
- 557 35. S.-P. Xie, H. Annamalai, F. A. Schott, Structure and mechanisms of south Indian Ocean
558 climate variability. *J. Clim.* **15**, 864–878 (2002).
- 559 36. Y. Du, S.-P. Xie, G. Huang, K. Hu, Role of air–sea interaction in the long persistence of El
560 Niño–induced north Indian Ocean warming. *J. Clim.* **22**, 2023–2038 (2009).
- 561 37. S.-P. Xie, Y. Kosaka, Y. Du, K. Hu, J. S. Chowdary, G. Huang, Indo-Western Pacific Ocean
562 capacitor and coherent climate anomalies in post-ENSO summer: a review. *Adv. Atmos.*
563 *Sci.* **33**, 411–432 (2016).
- 564 38. M. Ohba, H. Ueda, An impact of SST anomalies in the Indian Ocean in acceleration of the
565 El Niño to La Niña transition. *J. Meteor. Soc. Jap.* **85**, 335–348 (2007).
- 566 39. D. Dommenges, V. Semenov, M. Latif, Impacts of the tropical Indian and Atlantic Oceans
567 on ENSO. *Geophys. Res. Lett.* **33**, L11701 (2006).
- 568 40. Santoso, M. H. England, W. Cai, Impact of Indo-Pacific feedback interactions on ENSO
569 dynamics diagnosed using ensemble climate simulations. *J. Clim.* **25**, 7743–7763 (2012).
- 570 41. J. S. Kug, T. Li, S. I. An, I.S. Kang, J. J. Luo, S. Masson, T. Yamagata, Role of the ENSO–
571 Indian Ocean coupling on ENSO variability in a coupled GCM. *Geophys. Res. Lett.* **33**,
572 L09710. doi:10.1029/2005GL024916 (2006).

- 573 42. D. Dommenges, Y. Yu, The effects of remote SST forcings on ENSO dynamics, variability
574 and diversity. *Clim. Dyn.* **49**, 2605-2624 (2017).
- 575 43. T. Izumo, J. Vialard, H. Dayan, M. Lengaigne, I. Suresh, A simple estimation of equatorial
576 Pacific response from windstress to untangle Indian Ocean Dipole and Basin influences on
577 El Niño. *Clim Dyn.* **46**, 2247–2268 (2016).
- 578 44. K.-J. Ha, J.-E. Chu, J.-Y. Lee, K.-S. Yun, Interbasin coupling between the tropical Indian
579 and Pacific Ocean on interannual timescale: observation and CMIP5 reproduction. *Clim*
580 *Dyn.* **48**, 459–475 (2017).
- 581 45. W. Zhang, Y. Wang, F.-F. Jin, M. F. Stuecker, A. G. Turner, Impact of different El Niño
582 types on the El Niño/IOD relationship. *Geophys. Res. Lett.* **42**, 8570–8576 (2015).
- 583 46. T. Lee, M. J. McPhaden, Increasing intensity of El Niño in the central-equatorial Pacific.
584 *Geophys. Res. Lett.* **37**, L14603 (2010).
- 585 47. Y.-G. Ham, J.-Y. Choi, J.-S. Kug, The weakening of the ENSO–Indian Ocean Dipole (IOD)
586 coupling strength in recent decades. *Clim. Dyn.* **49**, 249–261 (2016).
- 587 48. Y. M. Okumura, C. Deser, Asymmetry in the duration of El Niño and La Niña. *J. Clim.* **23**,
588 5826–5843 (2010).
- 589 49. H. Annamalai, J. Potemra, R. Murtugudde, J. P. McCreary, Effect of Preconditioning on
590 the Extreme Climate Events in the Tropical Indian Ocean*. *J. Clim.* **18**, 3450–3469 (2005).
- 591 50. S.-K. Lee, W. Park, M. O. Baringer, A. L. Gordon, B. Huber, Y. Liu, Pacific origin of the
592 abrupt increase in Indian Ocean heat content during the warming hiatus. *Nat. Geo.* **8**, 445–
593 449 (2015).
- 594 51. M. F. Jansen, D. Dommenges, N. Keenlyside, Tropical atmosphere–ocean interactions in a
595 conceptual framework. *J. Clim.* **22**, 550-567 (2009).
- 596 52. C. Wang, F. Kucharski, R. Barimalala, A. Bracco, Teleconnections of the tropical Atlantic to
597 the tropical Indian and Pacific Oceans: A review of recent findings. Special Issue of
598 *Meteorologische Zeitschrift* **18**, 445-454 (2009).
- 599 53. C. Frauen, D. Dommenges, Influences of the tropical Indian and Atlantic Oceans on the
600 predictability of ENSO. *Geophys. Res. Lett.* **39**, L02706 (2012).

- 601 54. J. M. Wallace, D. S. Gutzler, Teleconnections in the geopotential height field during the
602 northern hemisphere winter. *Mon. Wea. Rev.* **109**, 784-812 (1981).
- 603 55. D. B. Enfield, D. A. Mayer, Tropical Atlantic sea surface temperature variability and its
604 relation to El Niño-Southern Oscillation. *J. Geophys. Res.* **102**, 929-945 (1997).
- 605 56. M. A. Alexander, I. Blade, M. Newman, J. R. Lanzante, N.-C. Lau, J. D. Scott, The
606 Atmospheric Bridge: The influence of ENSO teleconnections on air-sea interaction over the
607 global oceans. *J. Clim.* **15**, 2205-2231 (2002).
- 608 57. B. Huang, Remotely forced variability in the tropical Atlantic Ocean. *Clim. Dyn.* **23**, 133-
609 152 (2004).
- 610 58. C. Wang, "ENSO, Atlantic climate variability, and the Walker and Hadley circulations." in
611 *The Hadley Circulation: Present, Past and Future*, H. F. Diaz, R. S. Bradley, Eds. (vol. 21
612 of *Advances in Global Change Research Series*, Springer, Dordrecht, 2004), pp. 173-202.
- 613 59. J. Garcia-Serrano, C. Frankignoul, M. P. King, A. Arribas, Y. Gao, V. Guemas, D. Matei,
614 R. Msadek, W. Park, E. Sanchez-Gomez, Multi-model assessment of linkages between
615 eastern Arctic sea-ice variability and the Euro-Atlantic atmospheric circulation in current
616 climate. *Clim. Dyn.* **49**, 2407-2429 (2017).
- 617 60. J. C. H. Chiang, A. H. Sobel, Tropical tropospheric temperature variations caused by ENSO
618 and their influence on the remote tropical climate. *J. Clim.* **15**, 2616-2631 (2002).
- 619 61. J.-H. Yu, T. Li, Z. Tan, Z. Zhu, Effects of tropical North Atlantic SST on tropical cyclone
620 genesis in the western North Pacific. *Clim. Dyn.* **46**, 865-877 (2016).
- 621 62. J.-Y. Yu, S. T. Kim, Relationships between extratropical sea level pressure variations and
622 the central Pacific and eastern Pacific types of ENSO. *J. Clim.* **24**, 708–720 (2011).
- 623 63. S. E. Zebiak, Air-Sea interaction in the equatorial Atlantic region. *J. Clim.* **6**, 1567-1586
624 (1993).
- 625 64. N. S. Keenlyside, M. Latif, Understanding equatorial Atlantic interannual variability. *J.*
626 *Clim.* **20**, 131-142 (2007).
- 627 65. M. Latif, A. Grötzner, The equatorial Atlantic oscillation and its response to ENSO. *Clim.*
628 *Dyn.* **16**, 213-218 (2000).

- 629 66. P. Chang, Y. Fang, R. Saravanan, L. Ji, H. Seidel, The cause of the fragile relationship
630 between the Pacific El Niño and the Atlantic Niño. *Nature* **443**, 324-328 (2006).
- 631 67. J. F. Lübbecke, M. J. McPhaden, On the inconsistent relationship between Pacific and
632 Atlantic Niños. *J. Clim.* **25**, 4294-4303 (2012).
- 633 68. Polo, B. Rodríguez-Fonseca, T. Losada, J. Garcia-Serrano, Tropical Atlantic variability
634 modes (1979-2002). Part I: Time-evolving SST modes related to West African rainfall. *J.*
635 *Clim.* **21**, 6457-6475 (2008).
- 636 69. B. Rodríguez-Fonseca, I. Polo, J. García-Serrano, T. Losada, E. Mohino, C. R. Mechoso, F.
637 Kucharski, Are Atlantic Niños enhancing Pacific ENSO events in recent decades? *Geophys.*
638 *Res. Lett.* **36**, L20705 (2009).
- 639 70. H. Ding, N. S. Keenlyside, M. Latif, Impact of the equatorial Atlantic on the El Niño
640 Southern Oscillation. *Clim. Dyn.* **38**, 1965-1972 (2012).
- 641 71. Polo, M. Martín-Rey, B. Rodríguez-Fonseca, F. Kucharski, C. R. Mechoso, Processes in the
642 Pacific La Niña onset triggered by the Atlantic Niño. *Clim. Dyn.* **44**, 115-131 (2015).
- 643 72. M. Martín-Rey, B. Rodríguez-Fonseca, I. Polo, F. Kucharski, On the Atlantic–Pacific Niños
644 connection: a multidecadal modulated mode. *Clim. Dyn.* **43**, 3163-3178 (2014).
- 645 73. T. Losada, B. Rodriguez-Fonseca, Tropical atmospheric response to decadal changes in the
646 Atlantic equatorial mode. *Clim. Dyn.* **47**, 1211-1224 (2016).
- 647 74. M. Martín-Rey, I. Polo, B. Rodríguez-Fonseca, T. Losada, A. Lazar, Is there evidence of
648 changes in tropical Atlantic variability modes under AMO phases in the observational
649 record? *J. Clim.* **31**, 515-536 (2018).
- 650 75. B. Dong, R. T. Sutton, A. A. Scaife, Multidecadal modulation of El Niño-Southern
651 Oscillation (ENSO) variance by Atlantic Ocean sea surface temperatures. *Geophys. Res.*
652 *Lett.* **33**, L08705 (2006).
- 653 76. F. Kucharski, A. Bracco, J. H. Yoo, F. Molteni, Low-frequency variability of the Indian
654 monsoon–ENSO relationship and the tropical Atlantic: The “weakening” of the 1980s and
655 1990s. *J. Clim.* **20**, 4255-4266 (2007).
- 656 77. X. Rong, R. Zhang, T. Li, Impacts of Atlantic SST anomalies on the Indo-East Asian
657 summer monsoon-ENSO relationship. *Chin. Sci. Bull.* **55**, 1397-1408 (2010).

- 658 78. A. Gershunov, N. Schneider, T. Barnett, Low-Frequency Modulation of the ENSO–Indian
659 Monsoon Rainfall Relationship: Signal or Noise?. *J. Clim.* **14**, 2486–2492 (2001).
- 660 79. G. A. Meehl, J. M. Arblaster, J. T. Fasullo, A. Hu, K. E. Trenberth, Model-based evidence
661 of deep-ocean heat uptake during surface-temperature hiatus periods. *Nat. Clim.*
662 *Change* **1**, 360-364 (2011).
- 663 80. N. Maher, M. H. England, A. S. Gupta, P. Spence, Role of Pacific trade winds in driving
664 ocean temperatures during the recent slowdown and projections under a wind trend
665 reversal. *Clim. Dyn.* **51**, 321-336 (2018).
- 666 81. T. L. Delworth, F. Zeng, A. Rosati, G. A. Vecchi, A. T. Wittenberg, A link between the hiatus
667 in global warming and North American drought. *J. Clim.* **28**, 3834-3845 (2015).
- 668 82. W. Han, G. A. Meehl, A. Hu, M. Alexander, T. Yamagata, D. Yuan, M. Ishii, P. Pegion, J.
669 Zheng, B. Hamlington, X.-W. Quan, and R. Leben, Intensification of decadal and multi-
670 decadal sea level variability in the western tropical Pacific during recent decades. *Clim.*
671 *Dyn.* **43**, 1357-1379 (2014).
- 672 83. N. C. Johnson, S.-P. Xie, Changes in the sea surface temperature threshold for tropical
673 convection. *Nat. Geo.* **3**, 842-845 (2010).
- 674 84. L. Dong, M. J. McPhaden, Why has the relationship between Indian and Pacific Ocean
675 decadal variability changed in recent decades? *J. Clim.* **30**, 1971-1983 (2017).
- 676 85. R. Zhang, T. L. Delworth, Impact of the Atlantic multidecadal oscillation on North Pacific
677 climate variability. *Geophys. Res. Lett.* **34**, L23708 (2007).
- 678 86. C. Sun, F. Kucharski, J. Li, F.-F. Jin, I.-S. Kang, R. Ding, Western tropical Pacific
679 multidecadal variability forced by the Atlantic multidecadal oscillation. *Nat. Commun.* **8**,
680 15998 (2017).
- 681 87. Y. Ruprich-Robert, R. Msadek, F. Castruccio, S. Yeager, T. Delworth, G. Danabasoglu,
682 Assessing the climate impacts of the observed Atlantic multidecadal variability using the
683 GFDL CM2.1 and NCAR CESM1 global coupled models. *J. Clim.* **30**, 2785-2810 (2017).
- 684 88. Y. Chikamoto, A. Timmermann, J.-J. Luo, T. Mochizuki, M. Kimoto, M. Watanabe, M. Ishii,
685 S.-P. Xie, F.-F. Jin. Skillful multi-year predictions of tropical trans-basin climate
686 variability. *Nat. Commun.* **6**, 6869 (2015).

- 687 89. F. Kucharski, I.-S. Kang, R. Farneti, L. Feudale, Tropical Pacific response to 20th century
688 Atlantic warming. *Geophys. Res. Lett.* **38**, L03702 (2011).
- 689 90. F. Kucharski, F. Ikram, F. Molteni, R. Farneti, I.-S. Kang, H.-H. No, M. P. King, G.
690 Giuliani, K. Mogensen, Atlantic forcing of Pacific decadal variability. *Clim. Dyn.* **46**, 2337-
691 2351 (2016).
- 692 91. Y.-G. Ham, J.-S. Kug, J.-Y. Park, Two distinct roles of Atlantic SSTs in ENSO variability:
693 North tropical Atlantic SST and Atlantic Niño. *Geophys. Res. Lett.* **40**, 4012-4017 (2013).
- 694 92. R. T. Sutton, G. D. McCarthy, J. Robson, B. Sinha, A. T. Archibald, L. J. Gray, Atlantic
695 Multidecadal Variability and the U.K. ACSIS Program. *Bull. Amer. Meteor. Soc.* **99**, 415-
696 425 (2018).
- 697 93. F.-F. Jin, An equatorial ocean recharge paradigm for ENSO. Part I: Conceptual Model. *J.*
698 *Atmos. Sci.* **54**, 811-829 (1997).
- 699 94. C. S. Meinen, M. J. McPhaden, Observations of warm water volume changes in the
700 equatorial Pacific and their relationship to El Niño and La Niña. *J. Clim.* **13**, 3551-3559
701 (2000).
- 702 95. N. S. Keenlyside, H. Ding, M. Latif, Potential of equatorial Atlantic variability to enhance
703 El Niño prediction. *Geophys. Res. Lett.* **40**, 2278-2283 (2013).
- 704 96. J.-J. Luo, G. Liu, H. Hendon, O. Alves, T. Yamagata, Interbasin sources for two-year
705 predictability of the multi-year La Niña in 2010-2012. *Sci. Rep.* **7**, 2276 (2017).
- 706 97. M. J. McPhaden, M. Nagura, Indian Ocean dipole interpreted in terms of recharge
707 oscillator. *Clim. Dyn.* **42**, 1569-1586 (2014).
- 708 98. Y. Kushnir, W. Robinson, P. Chang, A. W. Robertson, The physical basis for predicting
709 Atlantic sector seasonal-to-interannual climate variability. *J. Clim.* **19**, 5949-5969 (2006).
- 710 99. Y. Chikamoto, M. Kimoto, M. Ishii, T. Mochizuki, T. T. Sakamoto, H. Tatebe, Y. Komuro,
711 N. Watanabe, T. Nozawa, H. Shiogama, M. Mori, S. Yasunaka, Y. Imada, An overview of
712 decadal climate predictability in a multi-model ensemble by climate model MIROC. *Clim.*
713 *Dyn.* **40**, 1201-1222 (2013).

- 714 100. D. Matei, J. Baehr, J. H. Jungclauss, W.A. Muller, J. Marotzke, Multiyear prediction
715 of monthly mean Atlantic Meridional Overturning Circulation at 26.5°N. *Science* **335**, 76-
716 79 (2012).
- 717 101. Y. Chikamoto, T. Mochizuki, A. Timmermann, M. Kimoto, M. Watanabe, Potential
718 tropical Atlantic impacts on Pacific decadal climate trends. *Geophys. Res. Lett.* **43**, 7143-
719 7151 (2016).
- 720 102. Y.-G. Ham, J.-S. Kug, Role of North Tropical Atlantic SST on the ENSO simulated
721 using CMIP3 and CMIP5 models. *Clim. Dyn.* **45**, 3103-3117 (2015).
- 722 103. J.-J. Luo, G. Wang, D. Dommenges, May common model biases reduce CMIP5's
723 ability to simulate the recent Pacific La Niña-like cooling? *Clim. Dyn.* **50**, 1335-1351 (2018).
- 724 104. W. Cai, A. Santoso, G. Wang, S.-W. Yeh, S.-I. An, K. M. Cobb, M. Collins, E.
725 Guilyardi, F.-F. Jin, J.-S. Kug, M. Lengaigne, M. J. McPhaden, K. Takahashi, A.
726 Timmermann, G. Vecchi, M. Watanabe, L. Wu, ENSO and greenhouse warming. *Nat. Clim.*
727 *Change* **5**, 849-859 (2015).
- 728 105. R. J. Small, E. Curchister, K. Hedstrom, B. Kauffman, W. G. Large, The Benguela
729 upwelling system: quantifying the sensitivity to resolution and coastal wind representation
730 in a global climate model. *J. Clim.* **28**, 9409-9432 (2015).

731 **Acknowledgments:** Special thanks to T.C. Soulik for noteworthy impact on an early draft of this
732 manuscript. We thank I. Polo and B. Rodriguez-Fonseca for helpful comments and suggestions,
733 and X. Hou for help with organization of the workshops. W.C., G.W., B.N., and A.S. are supported
734 by CSHOR and the Earth System and Climate Change Hub of the Australian Government's
735 National Environment Science Program. CSHOR is a joint research Centre for Southern
736 Hemisphere Oceans Research between QNLM and CSIRO. **Funding:** M.L. is supported by the
737 GOTHAM Belmont project (ANR-15-JCLI-0004-01) and the ARiSE ANR project. T.L. is supported
738 by NSFC 41630423 and NSF AGS-1565653 grants. S.M. is supported by Australian Research
739 Council (ARC) through grant number FT160100162. J.-S.K. was supported by the National
740 Research Foundation of Korea (NRF) grant funded by the Korea government (MSIT) (NRF-
741 2018R1A5A1024958). J.-Y.Y is supported by NSF AGS-1505145 and AGS-1833075 grants. M.F.S
742 is supported by the Institute for Basic Science (project code IBS-R028-D1). Y.-G.H. is funded by

743 the Korea Meteorological Administration Research and Development Program under grant
744 KMI2018-03214. M.J.M is supported by NOAA and PMEL contribution number 4838. Y.D. is
745 supported by the National Natural Science Foundation of China (41525019, 41830538, and
746 41521005) and the State Oceanic Administration of China (GASI-IPOVAI-02). D.D. is supported
747 by ARC grant number CE170100023. M.M.R. M.M.R. has been supported by the MORDICUS grant
748 under contract ANR-13-762 SENV-0002-01 and the CGL2017-86415-R. Y.R.-R. is supported by
749 800154-INADDEC individual MSCA-IF-EF-ST grant. S.-P.X. is supported by the National Science
750 Foundation. **Author contributions:** The manuscript was written as a group effort during two
751 ‘Pan-tropical inter-basin climate interactions’ workshops held at Xiamen University and Jeju
752 Island. All authors contributed to the manuscript preparation, interpretations and the discussions
753 that led to the final figure design. W.C. and L.W. designed the study and coordinated the writing.
754 M.L., T.L., S.M., J.-S.K., A.S., J.-Y.Y., X.L., M.F.S., Y.C., Y.-G.H., M.J.M., N.K., Y.R.-R., J.B.K.
755 coordinated the discussion for various sections. B.N. helped to collate comments and prepare an
756 initial version. **Competing interests:** The authors declare no competing interests. **Data and**
757 **materials availability:** All observation and model datasets used here are publicly available or on
758 request.

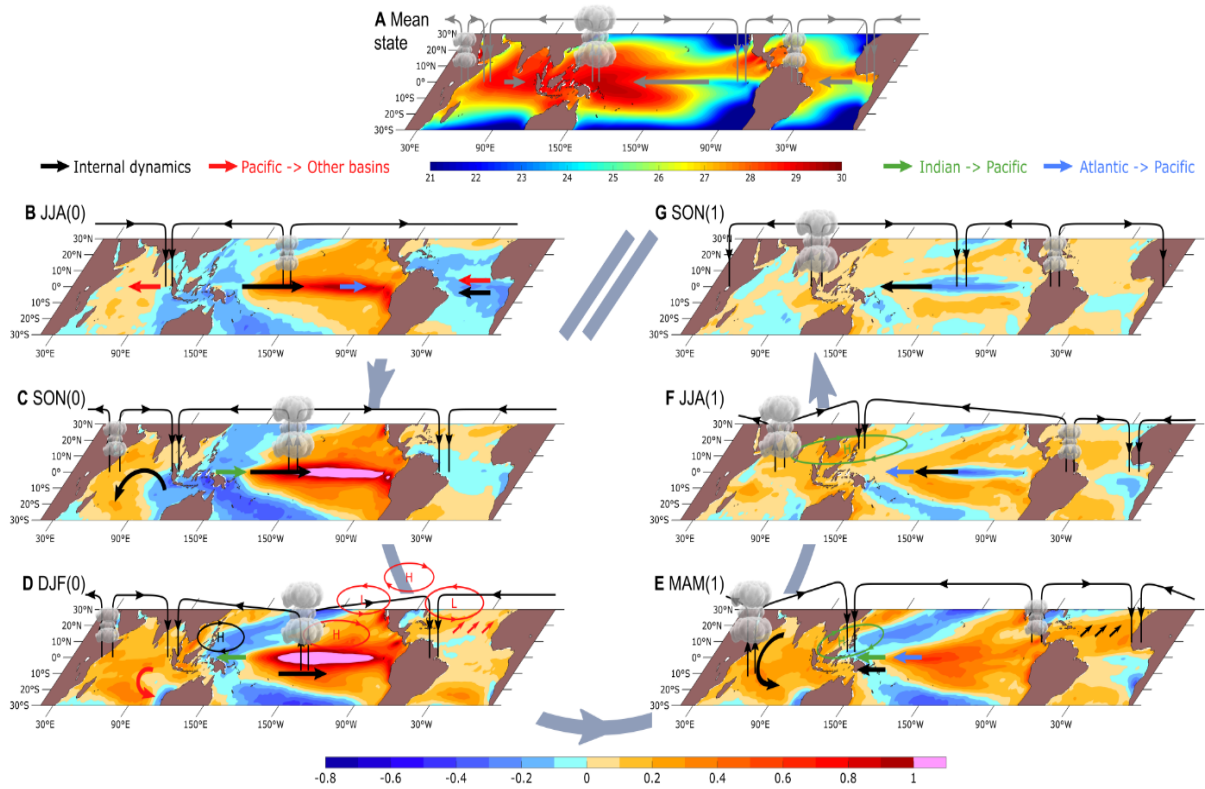
759

760

761

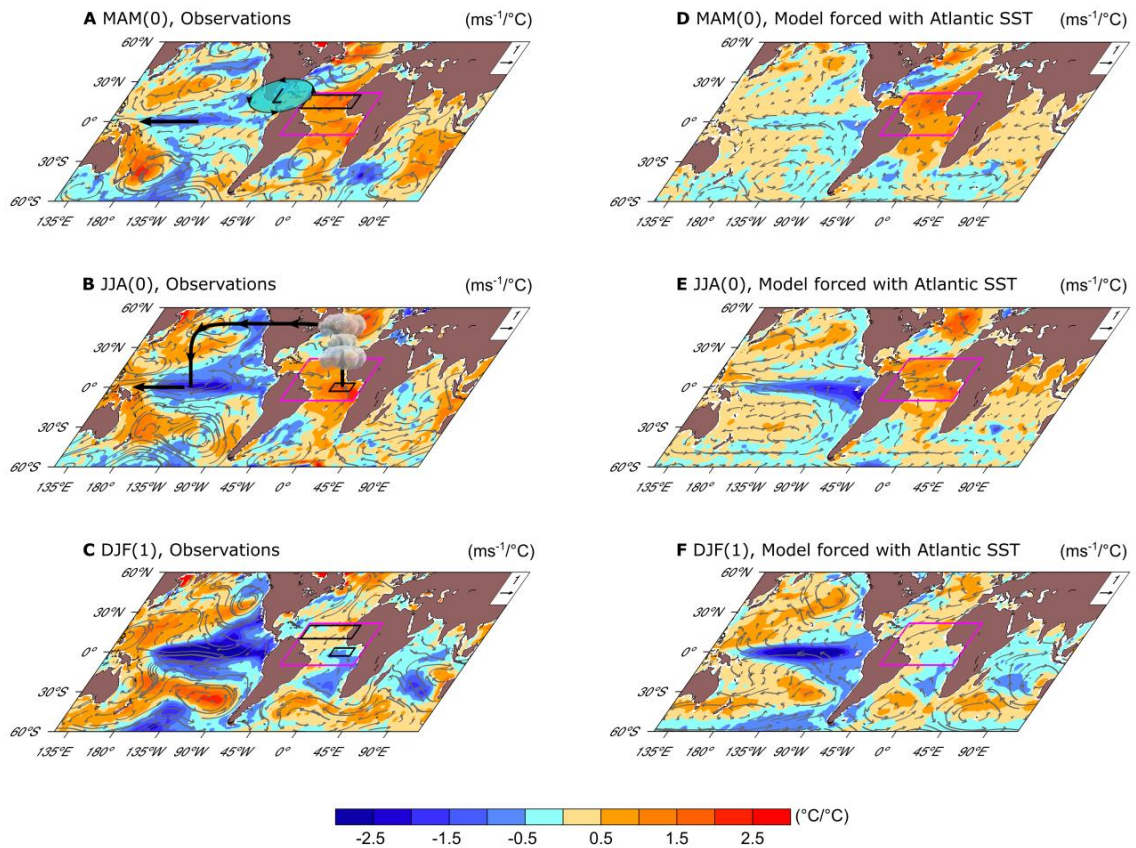
762

763



764

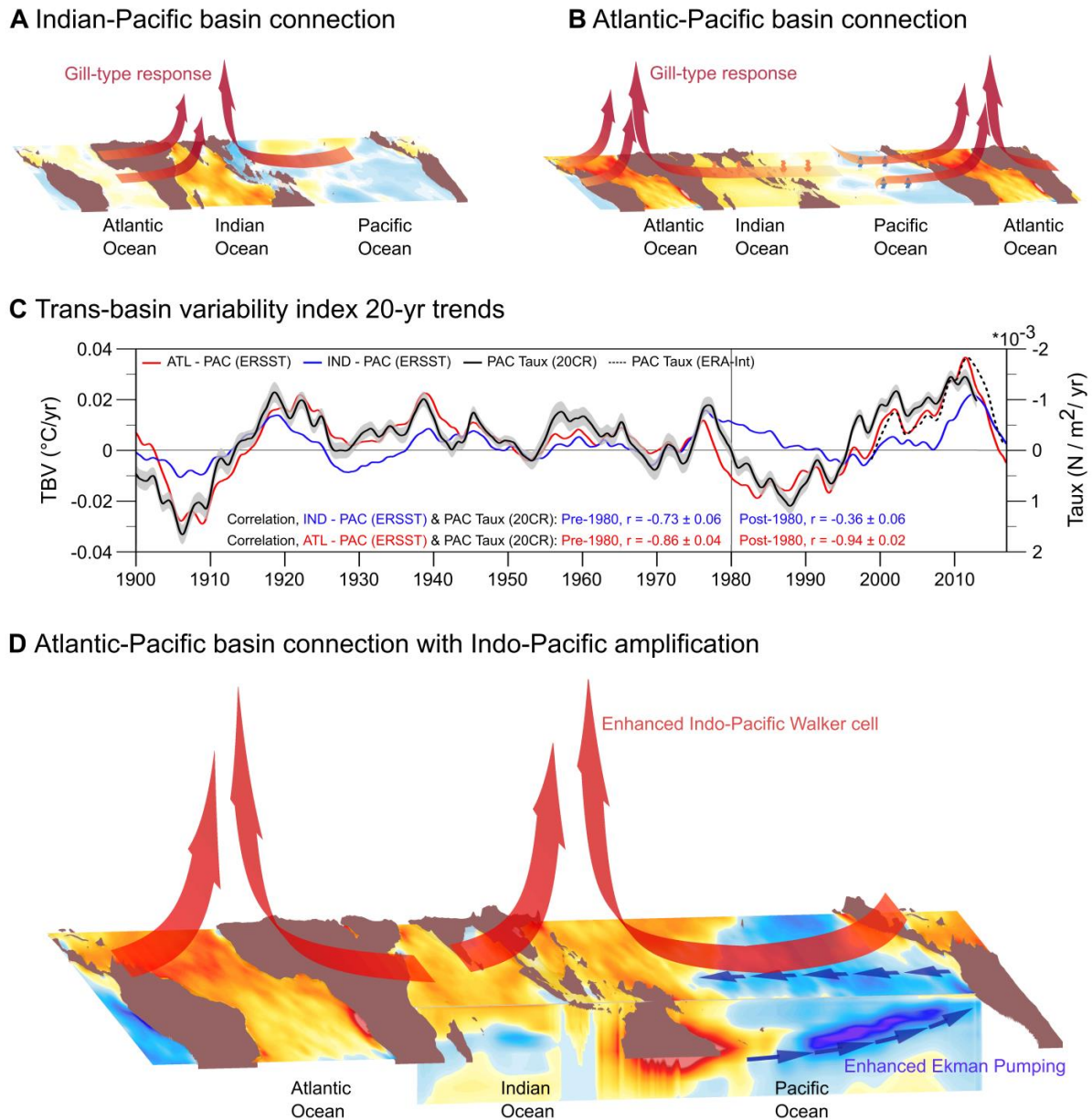
765 **Fig 1:** Evolution of tropical inter-basin interactions during a typical El Niño event. (A) Background
 766 mean state of SST (shading, [°C]) and Walker circulation (arrows). (B-G) Seasonally stratified SST
 767 anomaly lead/lag regression with normalized December-January-February (DJF) Niño3.4 (shading,
 768 [°C]) together with schematic surface wind and Walker Circulation changes (arrows). As El Niño
 769 grows, Walker Circulation changes lead to the development of (B-C) positive IOD, (D-E) IOB
 770 warming, (B) Atlantic Niña, and (D-E) NTA warming. (D-E) IOB and NTA warming induce
 771 equatorial wind anomalies in the Pacific, contributing to El Niño decay and transition to La Niña.
 772 (F) During post-El Niño summer, North Indian Ocean warming is coupled with the anomalous
 773 Northwest Pacific anticyclone, impacting Asian summer monsoon. Meanwhile, a developing La
 774 Niña in the Pacific favors Atlantic Niño conditions. The remaining seasons are abbreviated by
 775 March-April-May (MAM), June-July-August (JJA), and September-October-November (SON).
 776 Year 0 indicates an El Niño developing year, while year 1 indicates the subsequent decaying year.



777

778 **Fig. 2:** Tropical Atlantic influence on the Pacific. (A) Observed 1980-2005 SST and 850hPa wind
 779 anomalies in MAM(0) regressed onto a basin-wide SST index over the tropical Atlantic (10°S-20°N,
 780 60°W-10°E, purple box) in MAMJJA(0). This basin-wide index is selected to jointly capture the
 781 NTA (northern black box) and Atlantic Niño (southern black box) indices. The linear relation to
 782 the DJF(0) Nino3.4 index has been removed prior to the regression. NTA warming in MAM(0)
 783 generates a low-level cyclone over the eastern Pacific/Central America and easterly winds over the
 784 western equatorial Pacific through atmospheric Rossby and Kelvin wave responses. (B) In JJA(0),
 785 warming in the equatorial Atlantic induces anomalous Walker circulation, leading to anomalous
 786 easterlies in the central-western Pacific. (C) DJF(1), following the warming in the tropical Atlantic,
 787 cold anomalies develop in the central and eastern Pacific. (D-F) as in (A-C), but for a five member
 788 ensemble mean from pacemaker experiments performed over 1980-2005, in which full coupling is
 789 permitted everywhere except in the tropical Atlantic (30°S-30°N), where SSTs are nudged to
 790 observations (70).

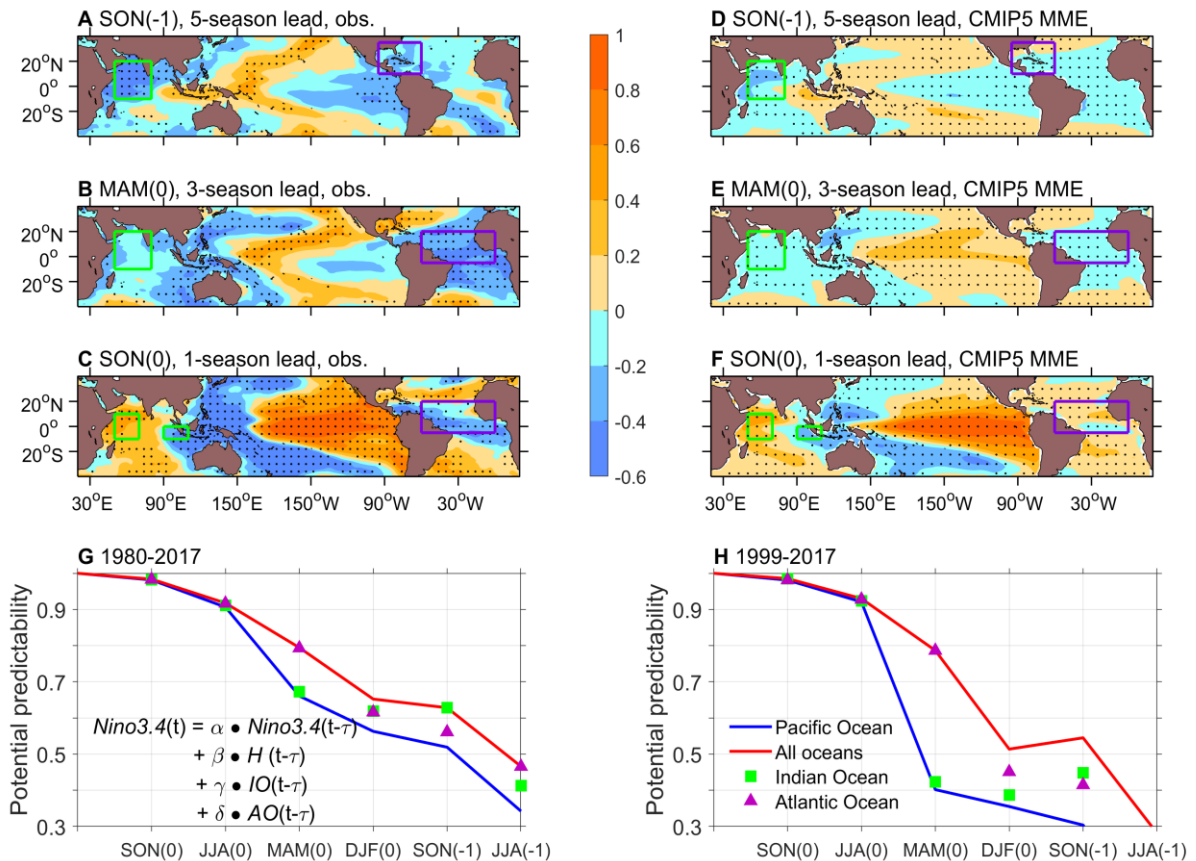
791



792

793 **Fig 3:** Decadal inter-basin connections with the Pacific. (A) Deep convection generated via Indian
 794 Ocean warming creates a Gill-type response that increases surface easterly winds and cold SSTs
 795 in the western Pacific. (B) Deep convection generated via Atlantic Ocean warming creates a Gill-
 796 type response, generating anomalous easterlies over the Indian Ocean and western Pacific. These
 797 anomalous winds lead to SST warming over the Indian Ocean and SST cooling over the
 798 western/central Pacific. The Gill-type response over the Atlantic also enhances the off-equatorial
 799 easterlies and cool SSTs in the eastern tropical Pacific. (C) Sliding window 20-year trends of inter-
 800 basin SST differences and equatorial western Pacific wind stress (recorded at end year of the

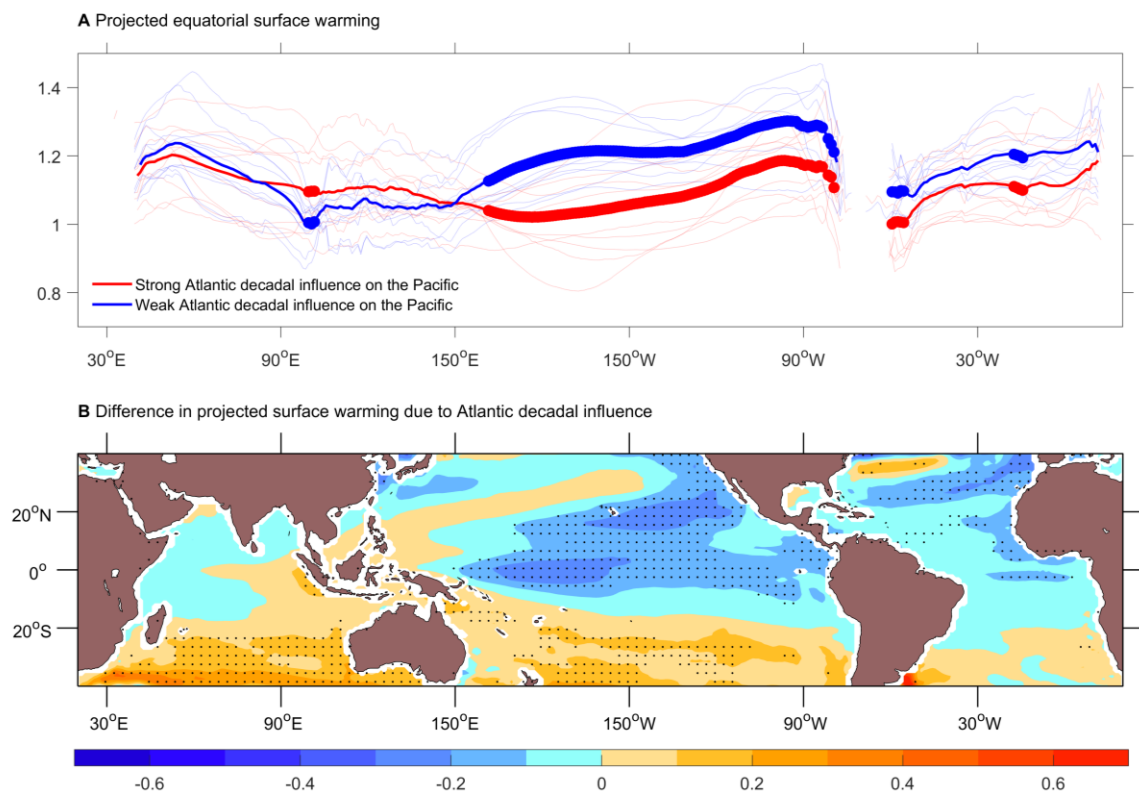
801 window). The wind stress and its one-standard deviation spread (shading) are from a 56-member
 802 reanalysis of the 20th century climate. Pre- and post-1980 correlations between the trans-basin SST
 803 and the ensemble-mean equatorial zonal wind trends are provided, together with one-standard
 804 deviation spread of correlations from the 56 realizations. Since 1980, the Atlantic-Pacific SST
 805 difference displays a stronger relationship with the Pacific winds than the Indian-Pacific SST
 806 difference. Indian, Pacific, and Atlantic basin SST are calculated between 20°S-20°N/21°E-120°E,
 807 20°S-20°N/121°E-90°W, and 20°S-20°N/70°W-20°E, respectively. The Pacific wind is computed
 808 between 6°S-6°N/180°E-210°E. **(D)** The atmospheric circulation and surface temperature changes
 809 generated due to Atlantic warming in **(B)** are amplified by the Pacific Bjerknes feedback **(Box 1)**
 810 and IOD-Pacific interactions. The depth-longitude section in **(D)** illustrates the subsurface
 811 temperature and circulation anomalies in the Indo-Pacific.
 812



813

814

815 **Fig 4:** Potential predictability of ENSO from inter-basin predictors. Lag correlation between
 816 November-December-January (NDJ) Niño3.4 SST and (A) 5-seasons preceding SST (SON), (B) 3-
 817 seasons preceding SST (MAM), and (C) 1-season preceding SST (SON) during the period of 1980-
 818 2017. Stippling in (A-C) indicates significant correlations at the 90% confidence level based on
 819 Student's t-test. Green and purple boxes in (A-C) denote the areas used for predictors of multiple
 820 regression in (G) and (H), for the respective seasons. The location of the green and purple boxes
 821 are chosen from areas with the strongest NDJ Niño3.4 correlation for each season. (D-F) as in (A-
 822 C), but for the ensemble mean of 43 CMIP5 models. Stippling in (D-F) indicates regions where 66%
 823 of models agree with the sign of the ensemble mean. Correlation between observed NDJ Niño3.4
 824 SST and reconstructed Niño3.4 SST from multiple regression with preceding predictors, as
 825 identified by strong regression coefficients, for the period of (G) 1980-2017 and (H) 1999-2017.
 826 Shown are results using internal Pacific predictors of western Pacific heat content (blue line),
 827 adding Indian Ocean (green squares), Atlantic (purple triangles), and both the Indian Ocean and
 828 the Atlantic Ocean predictors (red line).



829

830 **Fig. 5:** Impacts of model errors in decadal Atlantic-Pacific relationship on future climate
 831 projections. (A) Future projections of equatorial (5°S-5°N) SST (per degree of global warming) in

832 two ensembles of 10 CMIP5 models (thin curves) with a strong (red) and weak (blue) coupling
833 between decadal trends of an Atlantic-Pacific trans-basin variability index and equatorial Pacific
834 trade winds as in Ref. (18). Models with a stronger coupling tend to generate a weaker warming.
835 Changes are calculated as the difference in averages between the RCP8.5 2070-2099 and the
836 historical 1980-2009 period, divided by the global mean SST change over the same periods. The
837 broad thick curves denote where the difference between the two ensembles means (thick curves)
838 are significant at the 95% confidence level, based on Student's t-test. **(B)** Differences in
839 climatological SST changes between the two 10-model ensemble means. Stippling indicates areas
840 where the ensemble mean difference is significant at the 95% confidence level, based on a Student's
841 t-test.

842

843 **Box 1: Key Concepts Defined**

844 **Atlantic Multi-decadal Variability (AMV)** is a multi-decadal variation in sea surface
845 temperature, sometimes also referred to as the Atlantic Multi-decadal Oscillation (AMO). The
846 ultimate causes of this variability are the subject of ongoing research.

847 **Atlantic Niño and Niña** are generated along the equator in the Atlantic Ocean through ocean-
848 atmosphere interaction processes similar to those of ENSO, though they are weaker and shorter
849 lived than Pacific events.

850 **Atmospheric bridge** is a dynamical connection between tropical oceans that is associated with
851 variations of the Walker circulation.

852 **Atmospheric Kelvin wave** is an eastward propagating disturbance in the atmosphere. Kelvin
853 waves extend over the full height of the atmosphere, with a surface expression in the wind field
854 that affects ocean-atmosphere interactions.

855 **Atmospheric equatorial Rossby wave** is a westward propagating disturbance in the
856 atmosphere. Equatorial Rossby waves have a smaller zonal and larger meridional extent compared
857 to Kelvin waves and also affect the surface wind field and ocean-atmosphere interactions.

858 **Bjerknes feedback** is a positive feedback in which a weakened sea surface temperature gradient
859 along the equator leads to a weakening of the trade winds, which in turn further weakens the sea
860 surface temperature gradient. Equivalently, a strengthened sea surface temperature gradient
861 intensifies the trade winds, which then reinforce the surface temperature gradient.

862 **El Niño-Southern Oscillation (ENSO)** arises in the tropical Pacific through ocean-atmosphere
863 interactions involving Bjerknes feedback. It is the dominant mode of interannual climate
864 variability on the planet. El Niño events with their maximum sea surface temperature anomalies
865 in the eastern and central Pacific are referred to as EP El Niño and CP El Niño, respectively.

866 **Gill-type response** is a response to an equatorial heating anomaly, generating an equatorial
867 atmosphere Kelvin wave and associated surface easterly wind anomalies to its east, and
868 atmosphere Rossby waves and an associated pair of low pressure cells to its west, with cyclonic
869 surface westerly anomalies straddling the equator.

870 **Interdecadal Pacific Oscillation (IPO)** is a basin scale multi-decadal fluctuation in sea surface
871 temperature that is characterized in its positive phase by unusually warm tropics and cool
872 subtropics, and in its negative phase by opposite tendencies.

873 **Indian Ocean Basin (IOB) mode** is a uniform warming or cooling of the Indian Ocean that
874 occurs on interannual to decadal time scales.

875 **Indian Ocean Dipole (IOD)** is a mode of interannual variability in the tropical Indian Ocean
876 that arises from ocean-atmosphere interactions somewhat similar to those of ENSO, though IOD
877 events are weaker and shorter lived than ENSO events.

878 **North Tropical Atlantic (NTA)** is a sensitive region typically between 5°-20°N that both affects,
879 and is affected by, inter-basin interactions in the tropics.

880 **Walker circulation** is a series of zonal overturning cells in the atmosphere associated with
881 regions of rising and sinking motion.

882 **Wind-evaporation-SST (WES) effect** occurs when surface winds weaken over warm water,
883 which reduces evaporation and leads to further surface warming; or when surface winds
884 strengthen over cold water, enhancing evaporation and inducing further cooling. The sign of the
885 WES effect depends on whether the wind changes strengthen or weaken the mean winds.

886

887 **Enhanced Abstract**

888 **BACKGROUND**

889 Ocean-atmosphere interactions in the tropics have a profound influence on the climate system. El
890 Niño-Southern Oscillation (ENSO), which is spawned in the tropical Pacific, is the most prominent
891 and well-known year-to-year variation on Earth. Its reach is global and its impacts on society and
892 the environment are legion. Because ENSO is so strong, it can excite other modes of climate
893 variability in the Atlantic and Indian Oceans by altering the general circulation of the atmosphere.
894 However, ocean-atmosphere interactions internal to the Atlantic and Indian Oceans are capable of
895 generating unique modes of climate variability as well. Whether the Atlantic and Indian Oceans
896 can significantly feed back onto Pacific climate has been an ongoing matter of debate. We are now

897 beginning to realize that the tropics, as a whole, are a tightly interconnected system, with strong
898 feedbacks from the Indian Ocean and the Atlantic Ocean onto the Pacific. These two-way
899 interactions affect the character of ENSO and Pacific decadal variability and shed new light on the
900 recent hiatus in global warming. Here we review advances in our understanding of pan-tropical
901 inter-basin climate interactions and their implications for both climate prediction and future
902 climate projections.

903 **ADVANCES**

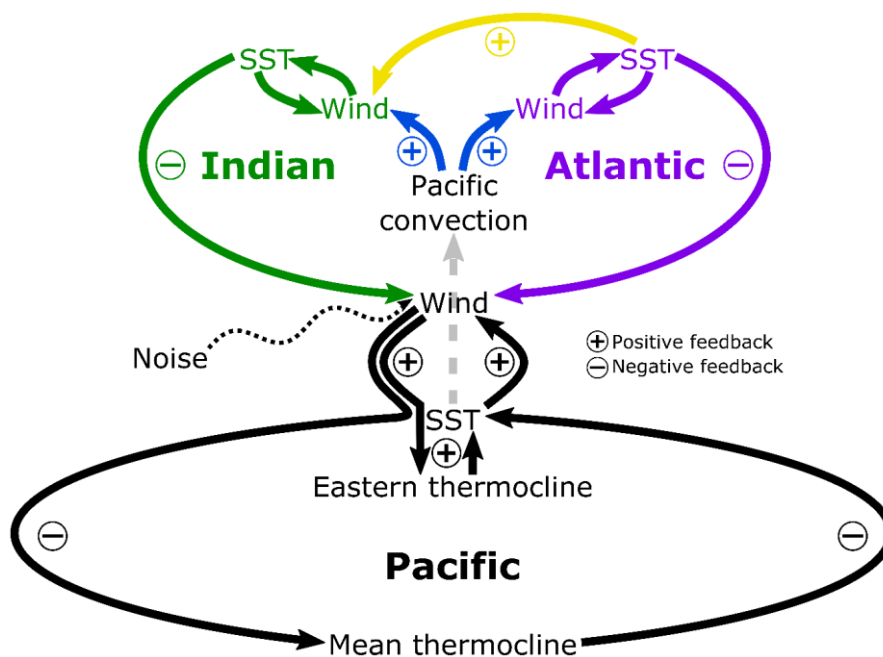
904 ENSO fluctuates between warm events (El Niño) and cold events (La Niña). These events force
905 changes in the Atlantic and Indian Oceans than can feedback onto the Pacific. Indian Ocean
906 variations, for example, can accelerate the demise of El Niño and facilitate its transition to La Niña.
907 ENSO events also exhibit significant diversity in their amplitude, spatial structure, and evolution,
908 which matters for how they impact on global climate. Sea surface temperature variations in the
909 equatorial and north tropical Atlantic can significantly contribute to the diversity of these events.
910 In addition, tropical inter-basin linkages vary on decadal time scales. Warming during a positive
911 phase of Atlantic Multi-decadal Variability (AMV) over the past two decades has strengthened the
912 Atlantic forcing of the Indo-Pacific, leading to an unprecedented intensification of the Pacific trade
913 winds, cooling of the tropical Pacific, and warming of the Indian Ocean. The Indo-Pacific
914 temperature contrast further strengthened the Pacific trade winds, helping to prolong the cooling
915 in the Pacific. These interactions forced from the tropical Atlantic were largely responsible for the
916 recent hiatus in global surface warming. Changes in Pacific mean state conditions during this
917 hiatus also significantly affected ENSO diversity.

918 **OUTLOOK**

919 There is tremendous potential for improving seasonal to decadal climate predictions and for
920 improving projections of future climate change in the tropics though advances in our
921 understanding of the dynamics that govern inter-basin linkages. The role of the tropical Atlantic
922 in particular requires special attention since all climate models exhibit systemic errors in the mean
923 state of the tropical Atlantic that compromise their reliability for use in studies of climate
924 variability and change. Projections based on the current generation of climate models suggest that

925 Pacific mean state changes in the future will involve faster warming in the east equatorial basin
 926 than the surrounding regions, leading to an increase in the frequency of extreme El Niños. Given
 927 the presumed strength of the Atlantic influence on the pan-tropics, projections of future climate
 928 change could be substantially different if model systematic errors in the Atlantic were corrected.
 929 Progress on these issues will depend critically on sustaining global climate observations, climate
 930 model improvements especially with regard to model biases, and theoretical developments that
 931 help us to better understand the underlying dynamics of pan-tropical interactions and their
 932 climatic impacts.

933



934

935 **Fig. 0:** Pan-tropical feedbacks affecting ENSO. Black loop represents internal Pacific fast positive
 936 feedbacks (short arrows) and delayed negative feedbacks (long arrows). Inter-basin feedbacks
 937 include Pacific feedbacks onto the Atlantic and Indian Oceans (blue arrows), delayed negative
 938 feedbacks of the Atlantic and Indian Oceans onto the Pacific (green/purple arrows) and positive
 939 feedbacks of the Atlantic onto the Indian Ocean (yellow arrow). The effects of atmospheric noise
 940 forcing in the Pacific is indicated by the dotted line.